DOI 10.31489/2022No4/5-16

UDC 537.636; 538.971; 539.22; 53.098

SPIN-SELECTIVE INTERACTION OF TRIPLET-EXCITED MOLECULES ON THE SURFACE OF A FERROMAGNETIC NANOPARTICLE

Kucherenko M.G., Neyasov P.P.*

Orenburg State University, Center for Laser and Information Biophysics, Orenburg, Russia, nejapetr@yandex.ru

Influence of a magnetic field generated by a ferromagnetic nanoparticle on the annihilation of triplet-excited organic molecules or triplet excitons in a near-surface particle layer is studied. A detailed mathematical model is presented that accounts for electron excitation diffusive mobility and geometry of the system. The kinetic operator is given in the complete 9x9 basis of triplet- triplet pair spin states. Time dependencies of the singlet spin state population of the triplet-triplet pair and the dependence of the triplet-triplet annihilation magnetic response profile (magnetic reaction effect) from the magnetic field induction are obtained. It is found that the influence of a magnetic field gradient on the reaction yield dominates over the other known mechanisms of spin-dynamics in triplet- triplet pairs.

Keywords: triplet-triplet annihilation, ferromagnetic nanoparticle, inhomogeneous magnetic field, magnetic effect.

Introduction

Contemporary studies of magnetically controlled processes in polymeric media, in particular, polymer light emitting diodes (PLEDs), present a special interest. For instance, paper [1] is devoted to the influence of an external magnetic field on the triplet-triplet annihilation (TTA) on the magnetically dependent electric conductivity (MEC) and on the magnetically dependent electroluminescence (MEL) of SY-PPV polymer (poly (para-phenylenevinylene)). In the present paper it is shown that in weak magnetic fields (<200 Oe) the positive magnetic effect occurs both for MEC and MEL. In magnetic fields H>200 Oe the decrease of MEL was explicitly observed; it is due to the increase of the triplet excitons lifetime and TTA suppression.

In paper [2] the influence of ferromagnetic $Co_{53}Pt_{47}$ nanowires induced in MEHPPV polymer (poly [2-methoxy,5-(2-ethylhexyloxy)-1,4-phenylenevinylene]) on electroluminescence was studied alongside the influence on phosphorescence of the iridium complex $Ir(ppy)_3$ (three-(2-phenylpyridinate) iridium (III)). Study performed in this paper shows that a doping with dispersed $Co_{53}Pt_{47}$ nanowires increases the probability of singlet-triplet exciton transitions in semiconductor MEHPPV films which are induced by the strong nanowires magnetic field. The influence of strong magnetic fields (B~9 T) on the magnetic fluorescence effect and phosphorescence in OLEDs was studied in [3].

Study of TTA involving electronically excited I_2-Bodipy molecules in various media was conducted in [4]. The influence of various solvent types on the quantum yield, delayed fluorescence frequency shift, and triplet states lifetime was studied. In paper [5] kinematics of the triplet excitation annihilation and the delayed fluorescence damping of an isolated 1,12-benzperylene pairs in n-hexane were studied; it was shown that their triplet excitation annihilation rate, decrease of the number of triplet-excited pairs, and damping of the annihilation delayed fluorescence are subjected to an exponential law provided the statistical spread of molecules by the rate constants vanishes. Exchange-resonance processes of homo- and heterogeneous annihilation of erythrosine and anthracene molecules placed on the surface of anodized aluminum were studied in a wide temperature interval [6]. The results show that the exchange photo-processes involving dye molecules adsorbed on the surface of anodized aluminum can be described within a fractal model. The direct influence of local magnetic fields of superparamagnetic Fe_2O_3 nanoparticles on the kinematics of the delayed fluorescence alongside 6G rhodamine and acriflavine fluorescence in the polyvinyl alcohol polymer matrix was empirically studied in [7].

Currently certain attempts to unite the descriptions of two physical processes, namely, plasmon resonance and TTA are conducted. In paper [8] an opportunity was studied to create a composite system for a photocatalytic destruction of an air pollutant, namely, acetaldehyde, based on the triplet-triplet annihilation which total photocatalytic efficiency is enhanced with plasmonic AgNP-SiO_2 nanoparticles. Plasmonic enhancement of the triplet-triplet annihilation within thin films of polymethylmethacrylate containing

.

palladium (II) octaethylporphyrin and 9,10-diphenylanthracene doped with silver nanoplates was found in [9]. The plasmon resonance allows one to detect fluorescence even if its intensity is extremely low. This fact was studied in details in paper [10]. Fluorescence of thin copper phthalocyanine on a golden platform was studied. The authors argued that the plasmon amplification of the triplet-triplet annihilation was also detected in the research.

Further studies of ferromagnetic particles influence on TTA in nanostructured media requires development of synthesis methods for such systems, for instance, nano-dispersed inclusions in the matrix can be polymer spheres [11-12]. These papers present a detailed discussion of ferromagnetic nanoparticles synthesis based on $FeCl_2$ and $FeCl_3$ electroless code position and their stabilization alongside the discussion of polymer spheres synthesis base on SAW (sodium dodecyl sulfate) and styrene. Nanoreactors are often synthesized on mesoporous silica base [13] and can also be based on ordered mesoporous carbon [14].

Paper [15] is devoted to a study of the pair spin states dynamics of two triplet (T) molecules which are partners in the spin-selective reaction and that were placed in a reaction cell with a ferromagnetic nanoparticle. It was taken into account that such a particle has residual magnetization, or acquires it in an external magnetic field. A theoretical model describing the T-T electronic perturbations annihilation in a nanoreactor containing a globular magnetic nanoparticle serving as the catalytic element was proposed and it is based on the so-called «Δg-mechanism» (which is due to the difference in molecules g-factors) which is due to a split of the cell volume in three areas divided by potential barriers. Within a strong field and hop reagent migration approximations it was evaluated how the magnetic annihilation effect value depends on the magnetic field induction generated by the catalytic nanoparticle in each of the spatially-separated areas.

Thus, despite the expressed interest in the problem of magnetically controlled annihilation of triplet electronic excitations near ferromagnetic nanoparticles, the analysis of the results obtained based on an adequate theoretical model of spin-selective reactions, which takes into account the inhomogeneous nature of the magnetic field in the vicinity of ferromagnetic nanoparticles, has not yet been carried out, due to the lack of such a model.

In this paper, a corresponding model is proposed and, on its basis, the spin dynamics of molecular T–T pairs in the magnetic field of a globular ferromagnetic nanoparticle is studied, taking into account the gradient effects of the field. In a typical variant of the migration of a spin-carrying molecule, i.e., its free diffusion in a circular or spherical region with a nanoparticle located in the center of the region and reflection at its boundary, the TTA magnetic effect was calculated from the modulation of the spin-selective reaction rate by the field. Moreover, in contrast to [15], the spin dynamics was analyzed in the general case, i.e., outside the framework of the strong magnetic field approximation. For this purpose, the 9x9 force matrix describing interactions between T-molecules is constructed (Table 1).

Giant palladium clusters have an icosahedral core with N=561 atoms (five-layer cluster). In a large number of works devoted to magnetic nanoclusters, clusters of spherical and spheroidal shapes are considered. Experimental observations of the shell structure of metal clusters show that clusters with a magic number of atoms have a spherical shape (N=13; 55; 147) [16]. Analysis of the rearrangement of the magnetization of Fe clusters at R>Rc was carried out for spherical clusters [17, 18].

1. Mathematical model

Magnetized ferromagnetic nanoparticle in a nanocavity creates a magnetic field that affects nearby spin-selective reactions involving paramagnetic molecules or triplet excitons. Be-cause of this it is important to search for a detailed description of the reaction kinematics in such nanoreactor systems with a magnetized core [15]. In this paper, we consider layered (shell) magnetic particles of a cylindrical or spherical shape, on the surface of which particles of two types (molecules or quasiparticles-excitons), with different diffusion coefficients D_1 and D_2, can freely move, annihilating at a distance is especially effective when they approach the interaction radius. Magnetic particles are placed inside nanoreactors.

The magnetic field arising in the shell does not significantly affect the nature of particle motion in the layer between the ferromagnetic particle and the inner surface of the nanoreactor. At the same time, the spin dynamics of molecules with a nonzero electronic or nuclear magnetic moment depends on the magnitude of the induction B of the magnetic field **B**.

In certain cases, spatial and spin dynamics can be studied independently. Nonetheless, the spin-selective annihilation yield is to be defined both by spatial and spin properties. In the case to be discussed further the

reaction rate depends on positions $\mathbf{r}_1$ and $\mathbf{r}_2$ of the reagents placed within the layer at a given time *t* which are "marked" with magnetic field induction vectors $\mathbf{B}(\mathbf{r}_1)$ and $\mathbf{B}(\mathbf{r}_2)$. We define the coordinate-spin density operator $\hat{\rho}(\mathbf{r}_1,\mathbf{r}_2,t\,|\,\mathbf{r}_1',\mathbf{r}_2',\mathbf{B}(\mathbf{r}_1),\mathbf{B}(\mathbf{r}_2))$ which defines the population growth rate of the state $|JM\rangle$ optimal for the reaction (here *J*, *M* are the total spin moment and its z-projection correspondingly). For the rate constant $K(\mathbf{r}_1',\mathbf{r}_2')$ of the spin-selective triplet (T) states annihilation the following holds

$$K(\mathbf{r}_1',\mathbf{r}_2')=\int_0^\infty dt\iint_{\Delta V_R}U(|\,\mathbf{r}_1-\mathbf{r}_2\,|)\frac{1}{2}\mathrm{Tr}\left\{\hat{P}_S,\hat{\rho}(\mathbf{r}_1,\mathbf{r}_2,t\,|\,\mathbf{r}_1',\mathbf{r}_2',\mathbf{B}(\mathbf{r}_1),\mathbf{B}(\mathbf{r}_2))\right\}_+ d^3r_1d^3r_2\,, \tag{1}$$

where $\mathrm{Tr}\left\{\hat{P}_S,\hat{\rho}\right\}_+=\sum_{J,M}\langle JM|\left(\hat{P}_S\hat{\rho}+\hat{\rho}\hat{P}_S\right)|JM\rangle=\langle 00|\hat{\rho}|00\rangle$, because $\hat{P}_S=|00\rangle\langle 00|$ is the operator performing a projection of the T-T pair singlet state; $\mathbf{r}_1',\mathbf{r}_2'$ are the initial positions of the mobile particles. ΔV_R - integration volume (volume of the layer between the ferromagnetic particle and the inner surface of the nanoreactor), $U(r)$ is the distance-dependent rate of an annihilation act. The spin-Hamiltonian of a T-T pair $\hat{H}(\mathbf{r}_1,\mathbf{r}_2)$ is given by the following

$$H=g_1\mu_B B(\mathbf{r}_1)S_{1Z}+g_2\mu_B B(\mathbf{r}_2)S_{2Z}-2J_{exc}(r_{12})\mathbf{S}_1\mathbf{S}_2-\mathbf{S}_1\mathbf{D}(\Omega_1)\mathbf{S}_1-\mathbf{S}_2\mathbf{D}(\Omega_2)\mathbf{S}_2\quad. \tag{2}$$

Description of the kinetic of the spin-selective triplet electronic excitations annihilation within a potential field $V(\mathbf{r}_1,\mathbf{r}_2)$ can be based on the density operator $\hat{\rho}(\mathbf{r}_1,\mathbf{r}_2,t)$ (we do not highlight here the explicit dependence on the magnetic field induction **B**, parameters $\mathbf{r}_1',\mathbf{r}_2'$ omitted) satisfying the following equation with the spin-Hamiltonian $\hat{H}(\mathbf{r}_1,\mathbf{r}_2)$ of the T-T pair and for the Fokker-Planck transport operator (the diffusion operators for a layer with the coefficient D_j)

$$\begin{aligned}\frac{\partial}{\partial t}\hat{\rho}(\mathbf{r}_1,\mathbf{r}_2,t)&=-\frac{i}{\hbar}\left[\hat{H}(\mathbf{r}_1,\mathbf{r}_2),\hat{\rho}(\mathbf{r}_1,\mathbf{r}_2,t)\right]-\Gamma\hat{\rho}(\mathbf{r}_1,\mathbf{r}_2,t)+\\&+\sum_{j=1}^{2}D_j\,\mathrm{div}\left(\nabla_j+\frac{1}{k_BT}\nabla_jV\right)\hat{\rho}(\mathbf{r}_1,\mathbf{r}_2,t)-\frac{1}{2}U(|\,\mathbf{r}_1-\mathbf{r}_2\,|)\left\{\hat{\rho}(\mathbf{r}_1,\mathbf{r}_2,t)\hat{P}_S+\hat{P}_S\hat{\rho}(\mathbf{r}_1,\mathbf{r}_2,t)\right\}.\end{aligned} \tag{3}$$

The first two terms define Zeeman interaction of single triplets (with different g-factors g_1 and g_2) of a T-T-pair with the local magnetic field induction $B(\mathbf{r}_j)$ generated by the ferromagnetic nanoparticle at the points of placement of molecules 1 and 2; the third term describes the intermolecular exchange interaction with the exchange $J_{exc}(r_{12})$ depending on the distance between triplet pairs r_{12}; the last two terms describe the inter-triplet spin-spin interaction. Operators S_1, S_2 are vector operators of molecules (1) and (2) electronic spins; $\mathbf{D}(\Omega_{1(2)})$ is the tensor of the magnetic dipole-dipole interaction; $\Omega_{1(2)}$ are the angular parameters; μ_B is the Bohr magneton. Hamiltonian of the spin-spin interaction $H_{SS}=-S_1D_1S_1-S_2D_2S_2$ accounts only for the magnetic dipole intermolecular interaction, while the inter-triplet spin-spin interaction is assumed to be negligibly small due to the relatively large radius of the molecular pair. The exchange interaction operator is diagonal in the pair basis $|JM\rangle$ of the total electronic spin of the T-T pair $S=S_1+S_2$. The value of the exchange integral fall with the intermolecular distance *r* and tends to zero in the following conditions $R_0<<r<R:\ J_{exc}(r)\to 0$.

In the case when the diffusion fluxes are determined by the density gradients of the initial distribution, and not by the gradients formed by distance annihilation, it can be assumed - at a sufficiently low annihilation rate - that diffusion occurs almost independently of the reaction. In that case the density operator $\hat{\rho}(\mathbf{r}_1,\mathbf{r}_2,t)$ can be factorized $\hat{\rho}(\mathbf{r}_1,\mathbf{r}_2,t)=\hat{\rho}_S(\mathbf{r}_1,\mathbf{r}_2,t)G_2(\mathbf{r}_1,\mathbf{r}_2,t)$, where $G_2(\mathbf{r}_1,\mathbf{r}_2,t)$ is the two-particle Fokker-Planck equation Green function for massless particles that do not interact with each other. Such a split of spatial and spin variables is justified be the following reasoning. The operator

$\hat{\rho}(\mathbf{r}_1,\mathbf{r}_2,t)=\hat{\rho}_S(\mathbf{r}_1,\mathbf{r}_2,t)G_2(\mathbf{r}_1,\mathbf{r}_2,t)$ can be placed into equation (2) and we are to assume that the following approximation holds

$$\sum_{j=1}^{2}D_j\nabla_j^2\hat{\rho}_S(\mathbf{r}_1,\mathbf{r}_2,t)G_2(\mathbf{r}_1,\mathbf{r}_2,t)\approx\hat{\rho}_S(\mathbf{r}_1,\mathbf{r}_2,t)\sum_{j=1}^{2}D_j\nabla_j^2G_2(\mathbf{r}_1,\mathbf{r}_2,t) \tag{4}$$

which is due to the small values of gradients $\nabla_j\hat{\rho}_S(\mathbf{r}_1,\mathbf{r}_2,t)$; therefore, the following inequalities hold

$$\sum_{j=1}^{2}D_j\nabla_j\hat{\rho}_S(\mathbf{r}_1,\mathbf{r}_2,t)\nabla_jG_2(\mathbf{r}_1,\mathbf{r}_2,t)<<\hat{\rho}_S(\mathbf{r}_1,\mathbf{r}_2,t)\sum_{j=1}^{2}D_j\nabla_j^2G_2(\mathbf{r}_1,\mathbf{r}_2,t)$$

and

$$G_2(\mathbf{r}_1,\mathbf{r}_2,t)\sum_{j=1}^{2}D_j\nabla_j^2\hat{\rho}_S(\mathbf{r}_1,\mathbf{r}_2,t)<<\hat{\rho}_S(\mathbf{r}_1,\mathbf{r}_2,t)\sum_{j=1}^{2}D_j\nabla_j^2G_2(\mathbf{r}_1,\mathbf{r}_2,t).$$

In that case equation (2) allows one to obtain the following equation for the spin-density operator $\hat{\rho}_S(\mathbf{r}_1,\mathbf{r}_2,t)$ which is free from the Laplacian and any other spatial derivatives

$$\begin{aligned}\frac{\partial}{\partial t}\hat{\rho}_S(\mathbf{r}_1,\mathbf{r}_2,t)=&-\frac{i}{\hbar}\left[\hat{H}(\mathbf{r}_1,\mathbf{r}_2),\hat{\rho}_S(\mathbf{r}_1,\mathbf{r}_2,t)\right]-\Gamma\hat{\rho}_S(\mathbf{r}_1,\mathbf{r}_2,t)-\\&-\frac{1}{2}U(|\mathbf{r}_1-\mathbf{r}_2|)\left\{\hat{\rho}_S(\mathbf{r}_1,\mathbf{r}_2,t)\hat{P}_S+\hat{P}_S\hat{\rho}_S(\mathbf{r}_1,\mathbf{r}_2,t)\right\}.\end{aligned} \tag{5}$$

In such a way the spatial variables $\mathbf{r}_1,\mathbf{r}_2$ in operator $\hat{\rho}_S(\mathbf{r}_1,\mathbf{r}_2,t)$ serve as parameters. Namely, in case of the triplet (T) excitations annihilation via the single channel the following holds

$$\hat{\rho}_S(\mathbf{r}_1,\mathbf{r}_2,t)=\exp[-\Gamma t]\exp(\hat{K}t)\hat{\rho}_S(\mathbf{r}_1',\mathbf{r}_2',0)\exp(\hat{K}^*t) \tag{6}$$

where are non-Hermitian evolution operators

$$\begin{aligned}\hat{K}(\mathbf{B}(\mathbf{r}_1),\mathbf{B}(\mathbf{r}_2))&=-\frac{i}{\hbar}\left(\hat{H}(\mathbf{B}(\mathbf{r}_1),\mathbf{B}(\mathbf{r}_2))-i\frac{\hbar}{2}\hat{\Lambda}(r_{12})\right),\\\hat{K}^*(\mathbf{B}(\mathbf{r}_1),\mathbf{B}(\mathbf{r}_2))&=\frac{i}{\hbar}\left(\hat{H}(\mathbf{B}(\mathbf{r}_1),\mathbf{B}(\mathbf{r}_2))+i\frac{\hbar}{2}\hat{\Lambda}(r_{12})\right).\end{aligned} \tag{7}$$

And the annihilation influence on the T-T pair spin-dynamics is explicitly accounted by the following operator

$$\hat{\Lambda}(r_{12})=U(|\mathbf{r}_1-\mathbf{r}_2|)\hat{P}_S.$$

The matrix $\langle JM|\hat{K}|J'M'\rangle$ of the kinetic operator (7) is given by the following Table 1. In the table 1: $H_Z^{\pm}=\mu_B\frac{i}{\hbar}(g_1B_1\pm g_2B_2)$ are Zeeman interaction matrix elements; $H_{exc}=2\frac{i}{\hbar}J_{exc}$ is the exchange interaction matrix element; $H_E^{\pm}=\frac{i}{\hbar}(E_1\pm E_2)$, $H_D^{\pm}=\frac{i}{\hbar}(D_1\pm D_2)$ are matrix elements of the spin-spin interaction.

We introduce the following notations $g_1=g$, $g_2=g+\Delta g$, $B_1=B$, $B_2=B+\Delta B$. In these notations the Hamiltonian (3) reads

$$\hat{H}=g\mu_BB\left(\hat{S}_{1Z}+\hat{S}_{2Z}\right)+\left[g\Delta B+\Delta g(B+\Delta B)\right]\mu_B\hat{S}_{2Z}-J_{exc}(r)\left(\hat{\mathbf{S}}^2-4\right)+\hat{V}_{SS}, \tag{3'}$$

or

$$\hat{H}=\hat{H}_0+V_{SS},\ \hat{H}_0=\hat{H}_0^{(1)}+\hat{H}_0^{(2)},\ \hat{H}_0^{(1)}=g\mu_BB\hat{S}_Z-J_{exc}(\hat{\mathbf{S}}^2-4),\ \hat{H}_0^{(2)}=[g\Delta B+\Delta g(B+\Delta B)]\mu_B\hat{S}_{2Z}.$$

Terms of Hamiltonian (3') should be grouped up as follows: $\hat{H} = \hat{H}_0^{(1)} + [\hat{H}_0^{(2)} + \hat{V}_{SS}] = \hat{H}_0^{(1)} + \hat{V}$. The pair basis sates $|JM\rangle$ are eigenstates for $\hat{H}_0^{(1)}$, but not for $\hat{H}_0^{(2)}$. Consequently,

$$\hat{H}_0^{(1)}|JM\rangle = \left[g\mu_B BM - J_{exc}\left(J(J+1)-4\right)\right]|JM\rangle,\ M = m_1 + m_2,$$

while operators $\hat{H}_0^{(2)}, \hat{V}_{SS}$ induce transitions between states of the pair basis $|JM\rangle$.

Table 1. The kinetic operator matrix $\langle JM|K|J'M'\rangle$

J \ J'		**0**	**1**			**2**				
	M \ M'	**0**	**-1**	**0**	**1**	**-2**	**-1**	**0**	**1**	**2**
0	**0**	$2H_{exc} - K_S$	0	$-\frac{2}{\sqrt{6}}H_Z^{\pm}$	0	$-\frac{1}{\sqrt{3}}H_E^{\pm}$	0	$-\frac{\sqrt{2}}{3}H_D^{\pm}$	0	$-\frac{1}{\sqrt{3}}H_E^{\pm}$
1	**-1**	0	$\frac{1}{2}H_Z^{\pm} + H_{exc} + (1/6)H_D^{\pm}$	0	$\frac{1}{2}H_E^{\pm}$	0	$\frac{1}{2}(H_D^{\pm} - H_Z^{\pm})$	0	$\frac{1}{2}H_E^{\pm}$	0
	0	$-\frac{2}{\sqrt{6}}H_Z^{\pm}$	0	$H_{exc} - \frac{1}{3}H_D^{\pm}$	0	$-\frac{1}{\sqrt{2}}H_E^{\pm}$	0	$-\frac{2\sqrt{3}}{6}H_Z^{\pm}$	0	$\frac{1}{\sqrt{2}}H_E^{\pm}$
	1	0	$\frac{1}{2}H_E^{\pm}$	0	$H_{exc} - \frac{1}{2}H_Z^{\pm} + (1/6)H_D^{\pm}$	0	$-\frac{1}{2}H_E^{\pm}$	0	$-\frac{1}{2}(H_Z^{\pm} + H_D^{\pm})$	0
2	**-2**	$-\frac{1}{\sqrt{3}}H_E^{\pm}$	0	$-\frac{1}{\sqrt{2}}H_E^{\pm}$	0	$H_Z^{\pm} - H_{exc} - (1/3)H_D^{\pm}$	0	$-\frac{1}{\sqrt{6}}H_E^{\pm}$	0	0
	-1	0	$\frac{1}{2}(H_D^{\pm} - H_Z^{\pm})$	0	$-\frac{1}{2}H_E^{\pm}$	0	$\frac{1}{2}H_Z^{\pm} - H_{exc} + (1/6)H_D^{\pm}$	0	$-\frac{1}{2}H_E^{\pm}$	0
	0	$-\frac{\sqrt{2}}{3}H_E^{\pm}$	0	$-\frac{2\sqrt{3}}{6}H_Z^{\pm}$	0	$-\frac{1}{\sqrt{6}}H_E^{\pm}$	0	$\frac{1}{3}H_D^{\pm} - H_{exc}$	0	$-\frac{1}{\sqrt{6}}H_E^{\pm}$
	1	0	$\frac{1}{2}H_E^{\pm}$	0	$-\frac{1}{2}(H_Z^{\pm} + H_D^{\pm})$	0	$-\frac{1}{2}H_E^{\pm}$	0	$\frac{1}{6}H_D^{\pm} - \frac{1}{2}H_Z^{\pm} - H_{exc}$	0
	2	$-\frac{1}{\sqrt{3}}H_E^{\pm}$	0	$\frac{1}{\sqrt{2}}H_E^{\pm}$	0	0	0	$-\frac{1}{\sqrt{6}}H_E^{\pm}$	0	$-H_Z^{\pm} - H_{exc} - (1/3)H_D^{\pm}$

A numerical realization of the solution (6) can be expressed through the following exponential operators' matrices $\langle JM|\exp(Kt)|J'M'\rangle$

$$\langle JM|\hat{\rho}_S(t)|J'M'\rangle = \\ = \exp(-K_{-1}t) \times \sum_{J''M''}\sum_{J'''M'''} \langle JM|\exp(Kt)|J''M''\rangle\langle J''M''|\hat{\rho}_S(0)|J'''M'''\rangle\langle J'''M'''|\exp(K^*t)|J'M'\rangle \cdot \quad (8)$$

For 9×9 basis $|JM\rangle$ the representation $\langle JM|\exp(Kt)|J'M'\rangle$ obtained via the Sylvester theorem can be constructed numerically when the matrix $\langle JM|K|J'M'\rangle$ eigenvalues are found.

Solution of the diffusive part of the problem is obtained via the kinetic equation for the time-dependent two-particle Green function $G_2(\mathbf{r}_1,\mathbf{r}_2,t)$ for the within layer free diffusion equation

$$\frac{\partial}{\partial t}G_2(\mathbf{r}_1,\mathbf{r}_2,t)=D_1\nabla_1^2G_2(\mathbf{r}_1,\mathbf{r}_2,t)+D_2\nabla_2^2G_2(\mathbf{r}_1,\mathbf{r}_2,t). \tag{9}$$

Here $\nabla^2_{1(2)}$ is the tree-dimensional Laplace operator in coordinates $\mathbf{r}_1(\mathbf{r}_2)$. Being near one of the boundaries (spherical or cylindrical surface), $S(R_1)$ or $S(R_2)$ the particle gets into other conditions for its annihilation with another particle, in comparison with the case of a region without boundaries for the analytical Green function $G_2(\mathbf{r}_1,\mathbf{r}_2,t)$ is a more sophisticated problem. The absence of the annihilation term in (9) reduces its applicability only to the weak annihilation case. The following inequality for the rate amplitude can server as a suitable criterion for the weak annihilation regime within the studied problem $U_0=\max U(r_{12}):\ U_0<<D_{1(2)}/R^2_{1(2)}$. When the inequality is satisfied, the equation for the two-point Green function $G_2(\mathbf{r}_1,\mathbf{r}_2,t)$ is spited in two independent diffusion equations for each particle. Consequently, the Green function $G_2^{(0)}(\mathbf{r}_1,\mathbf{r}_2,t)$ is factorized with respect to the particle's coordinates: $G_2^{(0)}(\mathbf{r}_1,\mathbf{r}_2,t)=G_1(\mathbf{r}_1,t)G_1(\mathbf{r}_2,t)$.

Within the spherical frame with the z-axis being co-oriented with the magnetic moment vector **M** defining axial field in the gap, the Green function $G_1(r,\theta,\varphi,t)$ of each annihilating particle has the form

$$G_1(r,\theta,\varphi,t\,|\,r',\theta',\varphi')=\frac{3}{4\pi(R_2^3-R_1^3)}+\sum_{n=1}^{\infty}\exp\left[-D\left(\lambda_k^{(0)}\right)^2t\right]\frac{Z_{1/2}\left(\lambda_n^{(0)}r\right)Z_{1/2}\left(\lambda_n^{(0)}r'\right)}{4\pi\sqrt{rr'}\int\limits_{R_1}^{R_2}rZ^2_{1/2}\left(\lambda_n^{(0)}r\right)dr}+$$

$$+\sum_{n,l=1}^{\infty}\sum_{m=0}^{l}\exp\left[-D\left(\lambda_n^{(l)}\right)^2t\right]\frac{(2l+1)}{2\pi}\frac{(l-m)!}{(l+m)!}\frac{Z_{l+1/2}\left(\lambda_n^{(l)}r\right)Z_{l+1/2}\left(\lambda_n^{(l)}r'\right)}{\sqrt{rr'}\int\limits_{R_1}^{R_2}rZ^2_{l+1/2}\left(\lambda_n^{(l)}r\right)dr}\times \tag{10}$$

$$\times P_l^m(\cos\theta)\cdot P_l^m(\cos\theta')\cos m(\varphi-\varphi'),$$

here $Z_{l+1/2}(\lambda_n^{(l)}r)$ is a combination of the Bessel function $J_{l+1/2}(x)$ $N_{l+1/2}(x)$ of a semi-half index *l*+1/2

$$Z_{l+1/2}(\lambda_n^{(l)}r)=\left[\lambda_n^{(l)}J'_{l+1/2}(\lambda_n^{(l)}R_1)-J_{l+1/2}(\lambda_n^{(l)}R_1)/(2R_1)\right]N_{l+1/2}(\lambda_n^{(l)}r)-$$
$$-\left[\lambda_n^{(l)}N'_{l+1/2}(\lambda_n^{(l)}R_1)-N_{l+1/2}(\lambda_n^{(l)}R_1)/(2R_1)\right]J_{l+1/2}(\lambda_n^{(l)}r).$$

$P_l^m(\cos\theta)$ is the Legendre polynomials; $\lambda_n^{(l)}$ are the positive roots of the equation $\lambda_n^{(l)}\cdot Z'_{l+1/2}(\lambda_n^{(l)}R_2)-Z_{l+1/2}(\lambda_n^{(l)}R_2)/(2R_2)=0$.

Calculations based on the diffusion Green function (10) are complicated, so for the sake of illustration we assume that the moving molecule placed in the nanoreactor makes it diffusion walk in a certain plain within a circular area α which is a nanocell section passing through its diameter (Fig. 1a). In the circular symmetry case, which is due when the Green function does not depend on the angle φ the following equation holds for the radial Green function $G_1(r,t\,|\,r')$ of two-dimensional diffusion walk

$$G_1(r,t\,|\,r')=\frac{1}{\pi R^2}\left\{1+\sum_{k=1}^{\infty}\exp\left[-\frac{D}{R^2}\left(\mu_k^{(0)}\right)^2t\right]\frac{J_0\left(\mu_k^{(0)}r/R\right)J_0\left(\mu_k^{(0)}r'/R\right)}{J_0^2\left(\mu_k^{(0)}\right)}\right\}. \tag{11}$$

Here $\mu_k^{(n)}$ are positive roots of the equation $J'_n(\mu_k^{(n)})=0$; $J_n(x)$ is the Bessel functions of the first kind.

When a solution for equation (9) for two-particle Green function $G_2(\mathbf{r}_1,\mathbf{r}_2,t)$ is obtained, then the spin-selective biomolecular reaction rate constant $K(\mathbf{r}_1',\mathbf{r}_2')$ can be evaluated as follows

$$K(\mathbf{r}_1',\mathbf{r}_2') = \int_0^\infty dt \iint_{\Delta V_R} U(|\mathbf{r}_1-\mathbf{r}_2|)\frac{1}{2}\mathrm{Tr}\left\{\hat{P}_S,\hat{\rho}(\mathbf{r}_1,\mathbf{r}_2,t\,|\,\mathbf{B}(\mathbf{r}_1),\mathbf{B}(\mathbf{r}_2))\right\}_+ G_1(\mathbf{r}_1,t\,|\,\mathbf{r}_1')G_1(\mathbf{r}_2,t\,|\,\mathbf{r}_2')d^3r_1d^3r_2. \quad (12)$$

Expression (12) provides an exact solution of the stated problem with the main emphasis on the influence of boundaries S_1, S_2 on the kinematics. Radius-vectors $\mathbf{r}_1',\mathbf{r}_2'$ in (12) define the initial positions of particles 1 and 2. Therefore, the specific rate $K(\mathbf{r}_1',\mathbf{r}_2')$ of the biomolecular reaction depends on the initial configuration of the particle pair $\mathbf{r}_1',\mathbf{r}_2'$. It was assumed that the T-T annihilation rate $U(|\mathbf{r}_1-\mathbf{r}_2|)$ in (12) is represented by subjected to the exponential law

$$U(|\mathbf{r}_1-\mathbf{r}_2|) = U_0\exp\left[-2\frac{|\mathbf{r}_1-\mathbf{r}_2|}{l}\right],$$

where l is the characteristic scale of the overlapping of interaction molecules electron shells.

2. Results and discussion

It is assumed that some porous media when wetting form a thin liquid layer impregnated with ferromagnetic particles due to the adhesion. This assumption allows one to create a model for two-dimensional diffusion walk of T-molecules in a circular region (Figure 1a) which simplifies further calculations. A magnetized ferromagnetic core creates a heterogeneous field within the nanostructure. To be exact, in the case of two-dimensional walk within a circular section α the nanoparticle magnetic field induction distribution reads $B_2(r) = B/r^3$ (Figure 1b).

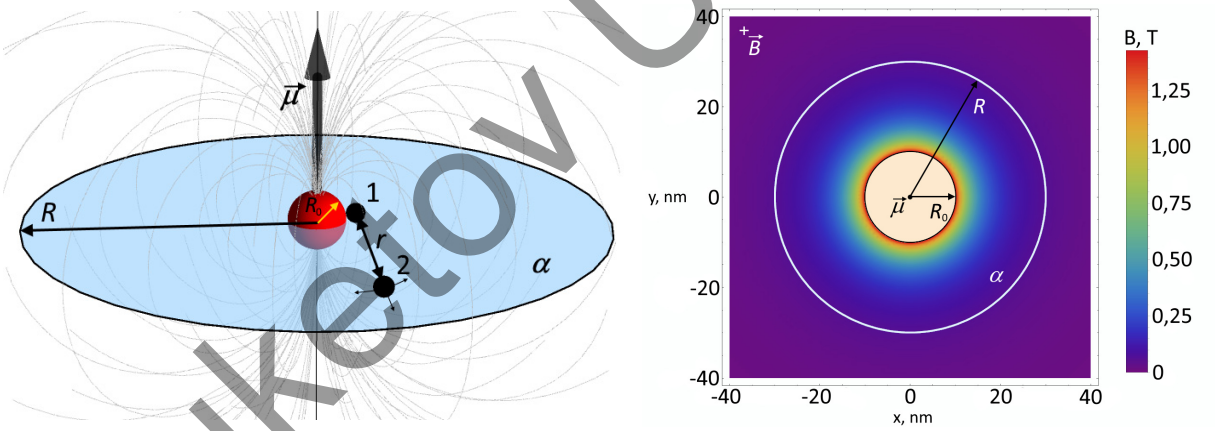

a) *b*)

Fig. 1. The structure of the studied system: the coherent T-T molecule pair-(1), (2) with the intermolecular distance r within a circular area α with the radius R containing a ferromagnetic particle in the center with the radius R_0 and the magnetic moment $\boldsymbol{\mu}$ ($\boldsymbol{\mu} = \mathbf{M}_0V$) (*a*); the distribution of the magnetic field induction B_2 generated by the ferromagnetic nanoparticle within the plane α given by $B_2(r) = B/r^3$ (*b*)

To study the influence of the ferromagnetic nanoparticle magnetic field (mainly, the influence which is due to the degree of its non-homogeneity) on the triplet-triplet excitation annihilation rate of excited molecules making diffusion walk in a proximity of such a particle we evaluated both space-time (Fig. 2) and time (Fig. 3-5) dependencies of the singlet matrix elements $\langle 00|\hat{\rho}_S(r,t)|00\rangle$ of the T-T pair spin density operator for various field values and molecular system parameters. Further we neglect the index S of the density operator $\hat{\rho}_S$, but we are to use indices *hom* or *het* to indicate homogeneity or heterogeneity of the field correspondingly. The radius r defines the position of the moving molecule with respect to the center of the nanoparticle. Heterogeneity of the magnetic field leads to the dependence of the population of the pair

singlet state $\langle 00|\rho_{het}(r,t)|00\rangle$ from the T-molecule coordinates. Results of calculations are presented on Fig. 2a and Fig. 2b. They show that the population is modulated by the T-molecule position both for weak residual fields $B < 0.1$ T (Fig. 2a) and for strong residual fields (> 0.1 T) (Fig. 2b). In weak heterogeneous fields the influence of the ΔB -mechanism weakens, so states $|2\pm1\rangle$ and $|1\pm1\rangle$ are mixed mainly because of the Δg -mechanism.

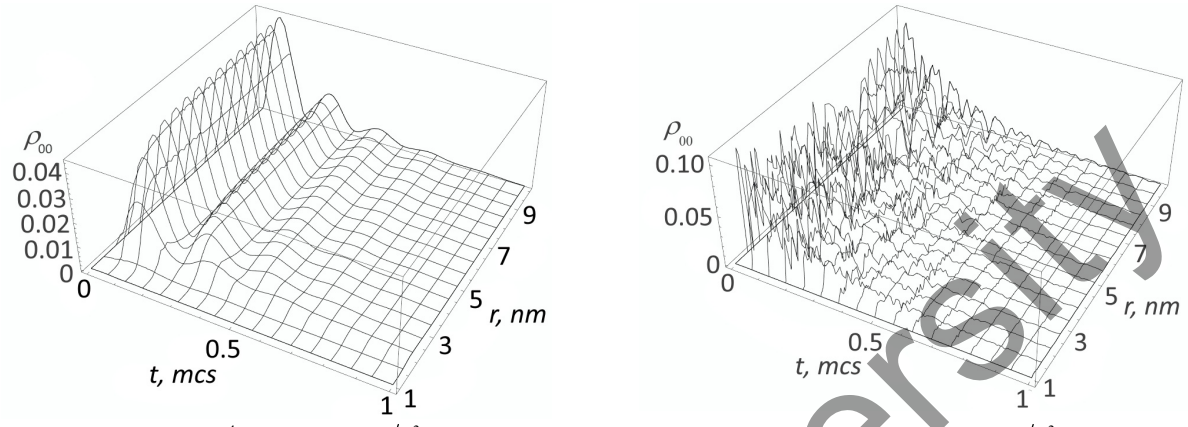

a) $B = 10^{-4}$ T, $B_2(r) = B/r^3$ *b*) $B = 0.1$ T, $B_2(r) = B/r^3$

Fig. 2. Evolution of the singlet T-T pair density population $\langle 00|\rho_{het}(r,t)|00\rangle = \rho_{00}$ placed in a residual magnetic field of the nanoparticle versus the position of the moving T-molecule. The following parameter values are used: $K_{-1} = 10^7$ s^{-1}, $\omega_{exc} = 10^7$ s^{-1}, $\Delta g = 10^{-3}$, $\omega_{ss}^{(1)} = 10^7$ s^{-1}, $\omega_{ss}^{(2)} = 2\cdot10^7$ s^{-1}, $K_s = 10^7$ s^{-1}

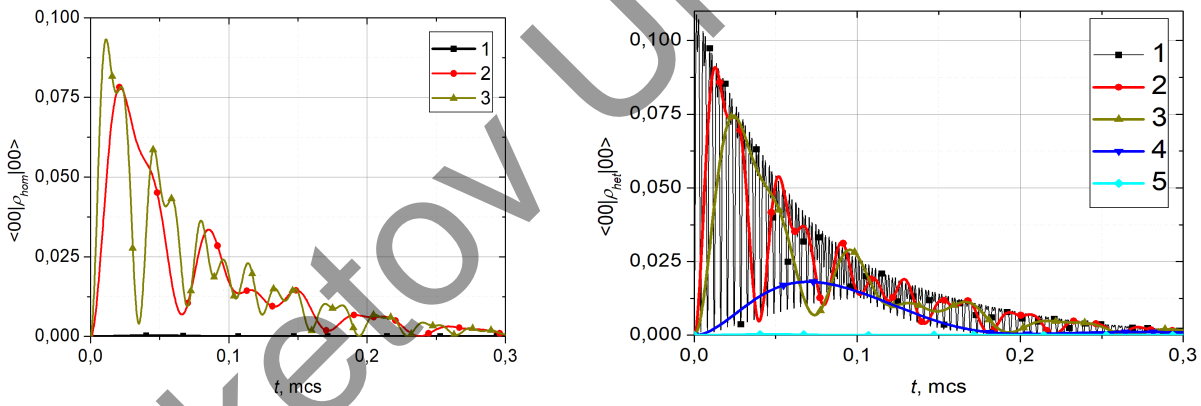

a) $B = B_2$: 0 (1), 1 (2) и 2 T (3) *b*) B: 10^{-2} (1), 10^{-3} (2), $5\cdot10^{-4}$ (3), 10^{-4} (4), 0 T (5); $B_2(r) = B/8$

Fig. 3. Kinetics of the singlet spin state population $\langle 00|\rho(r,t)|00\rangle$ of the T-T molecule pair at various values of the external magnetic field induction. (*a*) – non-magnetic nanoparticle, uniform magnetic field, (*b*) – ferromagnetic nanoparticle, inhomogeneous magnetic field. The following parameter values are used: $K_{-1} = 10^7$ s^{-1}, $\omega_{exc} = 10^7$ s^{-1}, $\Delta g = 10^{-3}$, $\omega_{ss}^{(1)} = 10^7$ s^{-1}, $\omega_{ss}^{(2)} = 2\cdot10^7$ s^{-1}, $K_s = 10^7$ s^{-1}, $r = 2$ nm

The existence of an external heterogeneous field **B** and its ΔB -mechanism influence result in a significant growth of the oscillation frequency of the pair singlet state population $\langle 00|\rho_{het}(r,t)|00\rangle$. This fact is well-illustrated with Figure 3. The population oscillation frequency within a homogeneous external field with induction 1-2 T is ~0,14-0,25 MHz (Fig. 3a), while in a heterogeneous field of weak induction B~10^{-2} T it rises up to ~ 24 MHz (Fig. 3b). The oscillation frequency for the case $\langle 00|\rho_{het}(r,t)|00\rangle$ matches the frequency for the case of a heterogeneous field with an amplitude B of the order of (~1) mT. Therefore, ΔB -mechanism results are a significant growth of the population oscillation frequency by 4-5 orders of magnitude.

The growth of the exchange frequency ω_{exc} in the generalized model accounting for the field heterogeneity describes previously unknown results, namely, the increase of the population probability of the pair singlet state $\langle 00|\rho(r,t)|00\rangle$ both for homogeneous and heterogeneous fields (Fig. 4). It also should be noted, that the increase of the exchange frequency ω_{exc} up to 10^9 Hz in case of $\langle 00|\rho_{het}(r,t)|00\rangle$ results in an insignificant fall of the amplitude (about 2,5 %), while $\langle 00|\rho_{hom}(r,t)|00\rangle \to 0$ due to the effective action of the ΔB -mechanism.

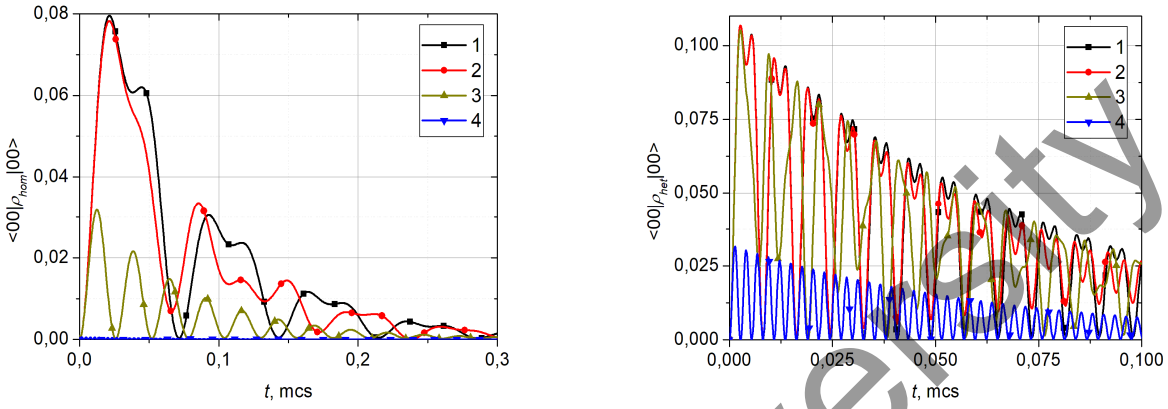

a) $B = B_2 = 1$ T; ω_{exc} : 10^6 (1), 10^7 (2), 10^8 (3), 10^9 (4) s^{-1}.

b) $B = 5 \cdot 10^{-3}$, $B_2(r) = 6{,}3 \cdot 10^{-4}$ T; ω_{exc} : 10^5 (1), 10^7 (2), 10^8 (3), 10^9 (4) s^{-1}.

Fig. 4. Kinetics of the spin singlet state population $\langle 00|\rho(r,t)|00\rangle$ of the T-T molecule pair at various values of the exchange frequency ω_{exc}. (*a*) – non-magnetic nanoparticle, uniform magnetic field, (*b*) – ferromagnetic nanoparticle, inhomogeneous magnetic field. The following parameter values are used: $K_{-1} = 10^7$ s^{-1}, $\Delta g = 10^{-3}$, $\omega_{ss}^{(1)} = 10^7$ s^{-1}, $\omega_{ss}^{(2)} = 2 \cdot 10^7$ s^{-1}, $K_s = 10^7$ s^{-1}, $r = 2$ nm

Elementary annihilation act rate K_s enters the matrix element $\langle JM|K|J'M'\rangle$ of the kinetic operator (Table 1). The increase of the rate K_s results in a decree of the amplitude of population $\langle 00|\rho(r,t)|00\rangle$ in an analogy with homogeneous (Fig. 5a) and heterogeneous magnetic field cases (Fig. 5b).

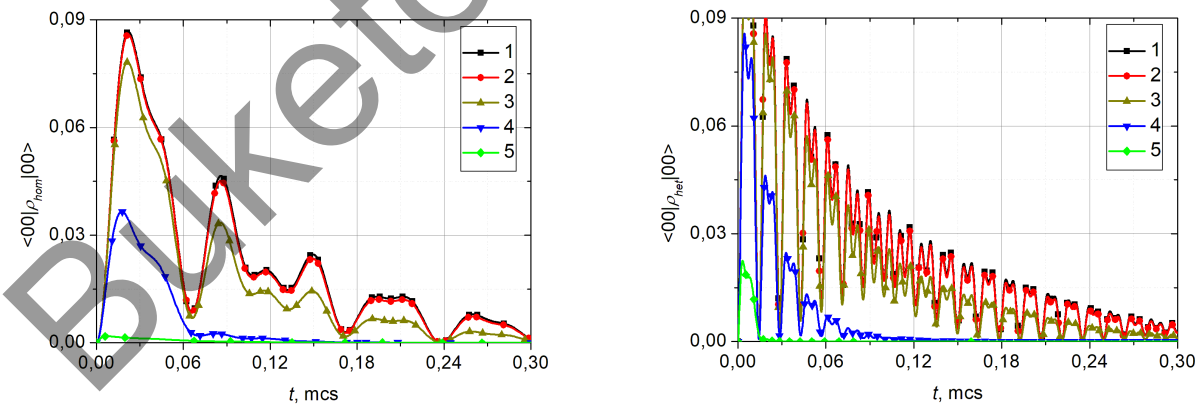

a) $B = B_2 = 1$ T; K_s : 10^5 (1), 10^6 (2), 10^7 (3), 10^8 (4), 10^9 (5) s^{-1}.

b) $B = 5 \cdot 10^{-3}$, $B_2(r) = 6{,}3 \cdot 10^{-4}$ T; K_s :10^5 (1), 10^6 (2), 10^7 (3), 10^8 (4), 10^9 (5) s^{-1}.

Fig. 5. Kinetics of the spin singlet state population $\langle 00|\rho(r,t)|00\rangle$ of the T-T molecule pair at various values of the elementary annihilation act rate K_s. (*a*) – non-magnetic nanoparticle, uniform magnetic field, (*b*) – ferromagnetic nanoparticle, inhomogeneous magnetic field. The following parameter values are used: $K_{-1} = 10^7$ s^{-1}, $\omega_{exc} = 10^7$ s^{-1}, $\Delta g = 10^{-3}$, $\omega_{ss}^{(1)} = 10^7$ s^{-1}, $\omega_{ss}^{(2)} = 2 \cdot 10^7$ s^{-1}, $r = 2$ nm

Moreover, calculations allow one to recover the dependency of the relative TTA (magnetic effect) rate change $\gamma(B)=[K(0)-K(B)]/K(0)$ from the magnetic field induction B (Fig. 6-8). The influence of the spin-spin interaction on the TTA reaction magnetic sensitivity results in a change of the interval where $\gamma(B)$ approaches asymptote (Fig. 6). This effect most clearly manifests itself in homogeneous fields (Fig. 6a). In a heterogeneous magnetic field, the effect is leveled out by the fast yield saturation due to the ΔB -mechanism (Fig. 6b). Figure 6 shows that the spin-spin interaction does not affect the form of curves $\gamma(B)$ for the frequencies $\omega_{ss}<10^7$ Hz. The modulation of the TTA reaction rate $\gamma(B)$ shows even more specific behavior in a proximity of either magnetic or non-magnetic nanoparticle when the T-molecules g-factor difference is changing (Fig. 7).

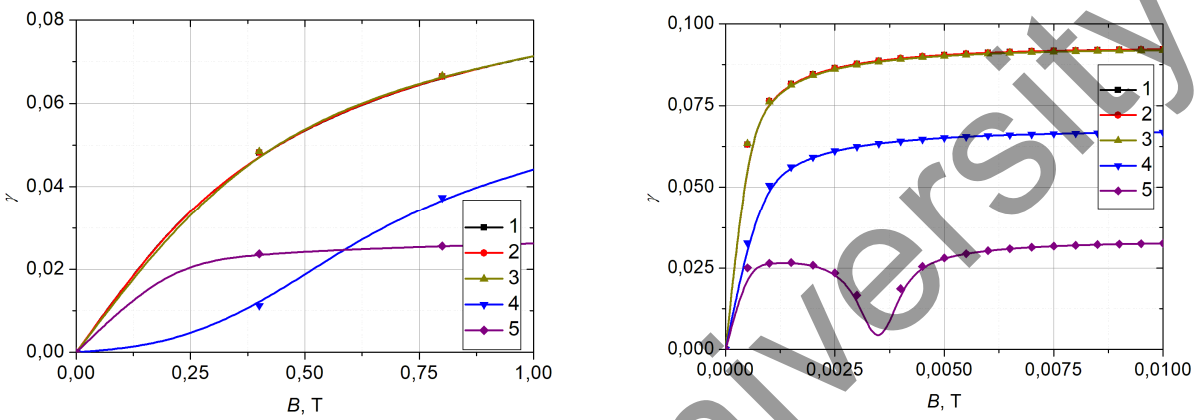

a) $B=B_2$; ω_{ss}: 10^5 (1), 10^6 (2), 10^7 (3), 10^8 (4), 10^9 (5) s^{-1}.

b) $B_2=B/r^3$; ω_{ss}: 10^5 (1), 10^6 (2), 10^7 (3), 10^8 (4), 10^9 (5) s^{-1}.

Fig. 6. The influence of the spin-spin interaction frequency ω_{ss} on the magnetic field effect $\gamma(B)$ within TTA reaction. (*a*) – non-magnetic nanoparticle, uniform magnetic field, (*b*) – ferromagnetic nanoparticle, inhomogeneous magnetic field. The following parameter values are used: $K_{-1}=10^7$ s^{-1}, $\omega_{exc}=10^7$ s^{-1}, $\Delta g=10^{-3}$, $K_s=10^7$ s^{-1}, $r'=2$ nm, $D=10^9$ nm^2/s, $R=10$ nm, $U_0=10^9$ s^{-1}, $r_0=0,5$ nm, $l=0,2$ nm, $a=0,99$

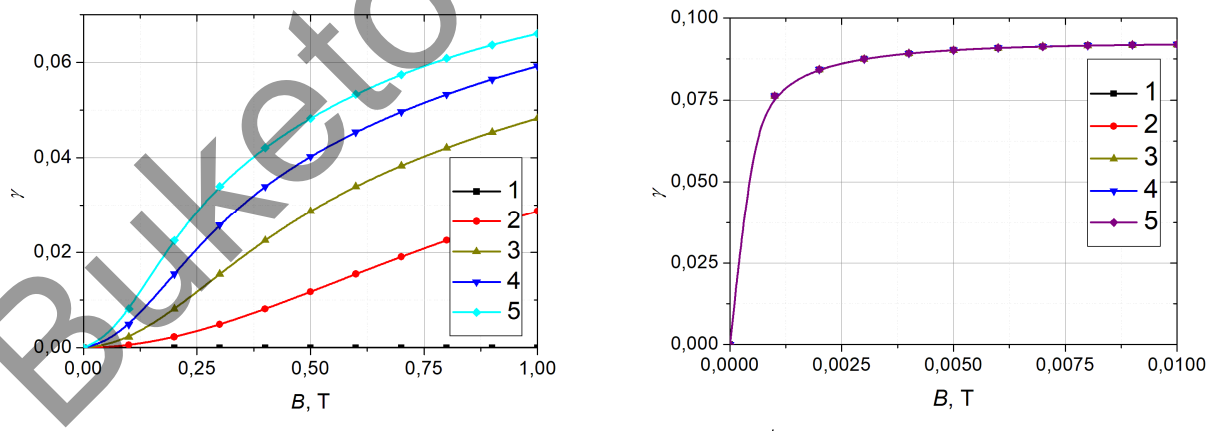

a) $B=B_2$; Δg: 0 (1), $2\cdot10^{-4}$ (2), $4\cdot10^{-4}$ (3), $6\cdot10^{-4}$ (4), $8\cdot10^{-4}$ (5)

b) $B_2=B/r^3$; Δg: 0 (1), $2\cdot10^{-4}$ (2), $4\cdot10^{-4}$ (3), $6\cdot10^{-4}$ (4), $8\cdot10^{-4}$ (5)

Fig. 7. The influence of the g-factors difference (Δg) of T-molecules on the magnetic field effect $\gamma(B)$ in TTA reaction. (*a*) – non-magnetic nanoparticle, uniform magnetic field, (*b*) – ferromagnetic nanoparticle, inhomogeneous magnetic field. The following parameter values are used: $K_{-1}=10^7$ s^{-1}, $\omega_{exc}=10^7$ s^{-1}, $\omega_{ss}^{(1)}=10^7$ s^{-1}, $K_s=10^7$ s^{-1}, $\omega_{ss}^{(2)}=2\cdot10^7$ s^{-1}, $r'=2$ nm, $D=10^9$ nm^2/s, $R=10$ nm, $U_0=10^9$ s^{-1}, $r_0=0,5$ nm, $l=0,2$ nm, $a=0,99$

In case of a heterogeneous magnetic field B_2 variations of Δg do not result in any observable changes for the magnetic effect $\gamma(B)$ (Fig. 7b). This feature is due to the suppressing action of the ΔB -mechanism in the presence of the weak Δg -mechanism. Diffusive Green functions (10)-(11) with reflective boundary conditions (at the boundary of the nanoreactor) were used for evaluation of the TTA reaction rate (12). Variations in the radius R of the nanoreactor circular area were the TTA processes occurs results in variations in the magnetic effect amplitude $\gamma(B)$ (Fig. 8). The spatial constraint of the T-molecules motion leads to their localization in the area of high magnetic field induction which, in turn, results in the increase of both reaction efficiency and magnetic response ($\gamma(B)$ ~26 %) in both cases.

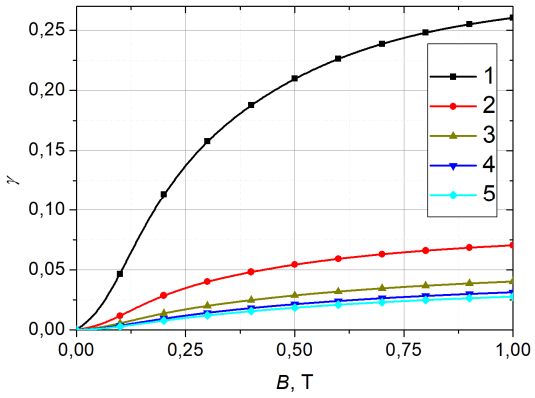

a) $B = B_2$; *R*: 5 (1), 10 (2), 15 (3), 20 (4), 25 (5) nm.

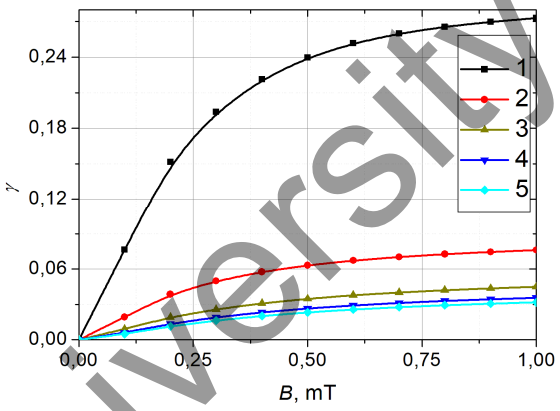

b) $B_2 = B/r^3$; *R*: 5 (1), 10 (2), 15 (3), 20 (4), 25 (5) nm.

Fig. 8. The influence of the radius *R* of the circular area α of the nanoreactor on the magnetic field effect $\gamma(B)$ in TTA reaction. (*a*) – non-magnetic nanoparticle, uniform magnetic field, (*b*) – ferromagnetic nanoparticle, inhomogeneous magnetic field. The following parameter values are used: $K_{-1} = 10^7$ s^{-1}, $\omega_{exc} = 10^7$ s^{-1}, $\Delta g = 10^{-3}$, $\omega_{ss}^{(1)} = 10^7$ s^{-1}, $\omega_{ss}^{(2)} = 2 \cdot 10^7$ s^{-1}, $K_s = 10^7$ s^{-1}, $r' = 2$ nm, $D = 10^9$ nm^2/s, $U_0 = 10^9$ s^{-1}, $r_0 = 0{,}5$ nm, $l = 0{,}2$ nm, $a = 0{,}99$

It should be noted that the increase of the radius *R* of the "reaction-diffusion" area alongside the diffusion coefficient *D* growth leads to a saturation of the reaction efficiency with respect to variation of *R* and *D*. This is due to the fact that the spin non-selective reaction rate rapidly approaches its asymptote and the T-T pairs spin dynamics remains relatively fast.

Conclusion

Magnetosensitivity of a reaction involving T-molecules in the most general case is affected by the inter-triplet electronic spin-spin interaction mechanism or the associated spin-relaxation mechanism. However, in the case of molecules high orientation mobility their chaotic reorientation can completely level out their anisotropic spin-spin interaction within the triplet. In an analogy with the spin radicals' case the reaction magnetic sensitivity can be driven by the Δg -mechanism of the magnetic response which is due to annihilation of T-molecules of various types. In homogeneous magnetic fields it can become the dominant factor generating the T-T pairs spin-dynamics. Consequently, within calculations of both pair singlet state population dynamics and the TTA specific rate magnetic effect we did account for the fine triplet energy structure associated with the spin-spin interaction operator $V_{SS} = -S_1 D_1 S_1 - S_2 D_2 S_2$ alongside the Δg -mechanism and the specific delta B-mechanism (or grad $B(\mathbf{r})$ -mechanism). To put it otherwise, the influence of the field heterogeneity on the T-T molecular pair dynamics was taken into account. It was shown that it is ΔB -mechanism that can effectively influence the singlet state $\langle 00|\rho(r,t)|00\rangle$ population dynamics of T-T molecular pair and lead to a positive TTA reaction magnetic response both for multi-sorted and single-sorted molecules (for which $\Delta g = 0$). In other words, in a heterogeneous magnetic field the ΔB -

mechanism replaces the Δg -mechanism in its influence of the magnetic field, as it provides the dominant contributions to the reaction rate magnetic response in nanostructures containing ferromagnetic particles.

REFERENCES

1 Nidya Ch., Ting-Yi Ch., Ping-Tsung H., Ten-Chin W., Tzung-Fang G. The triplet-triplet annihilation process of triplet to singlet excitons to fluorescence in polymer light-emitting diodes. *Organic Electronics*, 2018, Vol.62, pp.505-510. https://doi.org/10.1016/j.orgel.2018.06.021

2 Bin H., Yue W., Zongtau Zh., Sheng D., Jian Sh. Effects of ferromagnetic nanowires on singlet and triplet exciton fractions in fluorescent and phos-phorescent organic semiconductors. *Applied Physics Letters*, 2006, Vol. 88, pp. 022114. https://doi.org/10.1063/1.2162801

3 Toshihiro Sh. Effect of High Magnetic Field on Organic Light Emitting Diodes. *Organic Light Emitting Diode – Material, Process and Devices*, 2011, pp. 311-322. https://doi.org/10.5772/20743

4 Qiaohui Zh., Miaomiao Zh., Yaxiong W., Xiaoguo Zh., Shilin L., Song Zh., Bing Zh. Solvent effects on the triplet–triplet annihilation upconversion of diiodo-Bodipy and perylene. *Physical Chemistry Chemical Physics*, 2017, Vol. 19, pp. 1516-1525. https://doi.org/10.1039/C6CP06897A

5 Kolosov D.A., Deryabin M.I. Kinetics of annihilation of triplet excitations and decay of delayed fluorescence for isolated 1,12-benzoperylene pairs. *Journal of Applied Spectroscopy*, 2011, Vol. 78, No. 4, pp. 601-604. https://doi.org/10.1007/s10812-011-9504-z

6 Samusev I.G., Bruchanov V.V., Ivanov A.M., Labutin I.S., Loginov B.A. Heterogeneous triplet-triplet annihilation of erythrosine and anthracene molecules on a fractal anodized aluminum surface. *Journal of Applied Spectroscopy*, 2007, Vol. 74, No. 2, pp. 230-236. https://doi.org/10.1007/s10812-007-0036-5

7 Zarezin A.B., et al. Study of photophysical processes involving organic dye molecules and superparamagnetic nanoparticles in thin polymer films. *Kazan science*, 2011, No. 4, pp. 10-13. [in Russian]

8 Kim H., Weon S., Kang H., et al. Plasmon-Enhanced Sub-Bandgap Photocatalysis via Triplet–Triplet Annihilation Upconversion for Volatile Organic Compound Degradation. *Environmental Science & Technology*, 2016, Vol. 50, No. 20, pp. 11184-11192. https://doi.org/10.1021/acs.est.6b02729

9 Poorkazem K., Hesketh A.V., Kelly T.L. Plasmon-Enhanced Triplet–Triplet Annihilation Using Silver Nanoplates. *The Journal of Physical Chemistry C*, 2014, Vol. 118, No.12, pp. 6398-6404. https://doi.org/10.1021/jp412223m

10 Uemura T., Furumoto M., Nakano T., et al. Local-plasmon-enhanced up-conversion fluorescence from copper phthalocyanine. *Chemical Physics Letters*, 2007, Vol. 448, pp. 232-236. https://doi.org/10.1016/j.cplett.2007.09.084

11 Hervald A.Yu., Gritskova I.A., Prokopov N.I. Synthesis of magnetic-containing polymer microspheres. *Success of chemistry*, 2010, Vol. 79, No. 3, pp. 249-260. [in Russian]

12 Bronstein L.M., Sidorov S.N., Walecki P.M. Nanostructured polymer systems as nanoreactors for the formation of nanoparticles. *Success of chemistry*, 2004, Vol. 73, No. 5, pp. 542-558. [in Russian]

13 Mamoru M., Yuri Ya., Tadashi N., Kazuhisa Ya. Anomalous Pore Expansion of Highly Monodispersed Mesoporous Silica Spheres and Its Application to the Synthesis of Porous Ferromagnetic Composite. *Chemistry of Materials*, 2008, Vol. 20, No. 14, pp. 4777-4782. https://doi.org/10.1021/cm702792e

14 Jinwoo L., Sunmi J., Yosun H., Je-Geun P., Hyun Min P., Taeghwan H. Simple synthesis of mesoporous carbon with magnetic nanoparticles embedded in carbon rods. *Carbon*, 2005, Vol. 43, No. 12, pp. 2536-2543. https://doi.org/10.1016/j.carbon.2005.05.005

15 Kucherenko M.G., Neyasov P.P. Features of spin dynamics and annihilation of triplet molecular excitations in nanoreactors with ferromagnetic particles. *Chemical Physics and Mesoscopy*, 2018, Vol. 20, No. 1, pp. 33-48. [in Russian]

16 Heer W.A. de, Knight W.D., Chou M.Y., Cohen M.L. Electronic Shell Structure and Metal Cluster. *Solid State Physics*, 1987, Vol. 40, pp. 93-181. https://doi.org/10.1016/S0081-1947(08)60691-8

17 Afanas'ev A.M., Suzdalev I.P., Gen M. Ya., et al. Investigation of super-paramagnetism of ferromagnetic particles by Mossbauer spectroscopy. *Soviet Physics Jetp*, 1970, Vol. 31, No. 1, pp. 65-69.

18 Amulyavichu A.P., Suzdalev I.P. Investigation of the superparamagnetic properties of ultrafine iron particles by Mossbauer spectroscopy. *Zh. Eksp. Teor. Fiz,.* Vol. 64, pp. 1702-1711.

Article accepted for publication 30.11.2022